Pressures Developed during the Unidirectional Freezing of Water-Saturated Porous Materials

Experiment and Theory

Edward PENNER

Soil Mechanics Section, Division of Building Research
National Research Council, Ottawa, Ontario, Canada

Abstract

A new experimental apparatus is being used that permits the measurement of developing pressures during the freezing process in the environment of a small temperature gradient. Studies with pads of nearly uniform-size glass beads (in the micron range) indicate that after an ice lens has developed the ice-water interfacial energy, computed from the measured pressures and the pore geometry of glass bead pads, ranges between 30 and 35 ergs/cm^2. The supporting theory assumes that such pressures arise because of the curved interfaces between the ice lens and water, ice and porous solid, and water and solid according to Everett's model.

Freezing experiments with pads of well-graded spheres (1–30 μ) show the significance of the smaller pores in the porous system in determining the magnitude of pressures developed during ice lens growth. The study has been extended to soils and some common building materials.

I. Introduction

Frost heave experiments show that pressures developed at an ice-water boundary beneath an ice lens are related to the pore dimensions of the soil (Penner, 1958, 1963). In the absence of all confining pressures, the maximum suction (negative pressure) is developed in the water phase if the porous system does not have access to an external water supply. This suction is also related to the pore dimensions (Penner, 1957). It is possible also to halt ice lensing by a combination of suction and confining pressure (Penner, 1958).

The geometry of most porous materials is normally too complex for the investigation of theories that predict a precise relation between the heaving pressure induced by ice lensing and the geometry of the solid structure with its attendant pore system. The present paper describes freezing experiments with glass beads (which have only a small size variation and are in a close-pack array) to test more rigorously than has been done previously the prediction of heaving pressures by Everett and Haynes (1965). Based on the experimental technique devised and the agreement shown between theory and experiment, the studies have been extended to more complex porous systems, which contain a wide range in pore size distribution, in order to ascertain the significance of this size distribution on ultimate pressures. Such studies have been conducted in a preliminary way on a silty soil of known frost heave characteristics, on bricks, a cement mortar, and a sandstone.

II. Theory

The temperature at which ice will propagate through a pore restriction of given size in a water-saturated porous medium is given by the following equation (Sill and Skapski, 1956), provided the suction in the water is zero:

$$T - T_m = \Delta T = \frac{-2T_m\sigma_{iw}}{Q_f\rho_i r_i}, \tag{1}$$

where

r_i is radius of curvature of the ice-water interface and also pore radius,
ρ_i density of the ice,
Q_f latent heat of fusion,
T_m temperature of melting at zero curvature of the solid-liquid interface at standard pressure,
T temperature at which freezing takes place with radius of curvature, r, in contact with water,
σ_{iw} ice-water interfacial energy.

Everett and Haynes (1965) have predicted heaving pressures in porous materials based on pore size, the parameter used previously by others (Penner, 1957, 1958, 1963) with the important addition that the geometry of the systems is defined precisely. The case of special interest in the present paper is the close-pack array of uniform-size spheres (Everett and Haynes, 1965). This porous body is overlain by a continuous ice lens, as depicted in the schematic drawing of Fig. 1 a and b.

The pressure difference across the ice-water interface is given by

$$p^i - p^w = \frac{2\sigma_{iw}}{r_i}, \tag{2}$$

where

r_i is radius of curvature of the ice-water interface,
p^i pressure on the ice,
p^w pressure in the water,
and σ_{iw} interfacial energy term.

The pressure difference across the ice-solid interface at A is given by

$$p^i - p^s = \frac{-2\sigma_{is}}{r}, \tag{3}$$

where r is the radius of curvature of the solid.

Comparing eqs. (2) and (3) gives the pressure at point A as

$$p^s_A = p^w + \frac{2\sigma_{iw}}{r_i} + \frac{2\sigma_{is}}{r}. \tag{4}$$

In the region of the water-solid interface at B

$$p^s_B = p^w + \frac{2\sigma_{ws}}{r}. \tag{5}$$

The pressure difference across the region of the three-phase contact, if A and B are

brought close to C, is given by

$$\Delta p = p_A^s - p_B^s = \frac{2\sigma_{iw}}{r_i} + \frac{2}{r}(\sigma_{is} - \sigma_{ws}) . \quad (6)$$

Introducting the Young-Dupre equation

$$\sigma_{is} - \sigma_{ws} = \sigma_{iw} \cos\theta , \quad (7)$$

and defining B' as $\frac{r}{r_i}\frac{1}{\cos\theta}$, eq. (6) may be rewritten in the form

$$\Delta p = \frac{2\sigma_{iw}\cos\theta(1+B')}{r} . \quad (8)$$

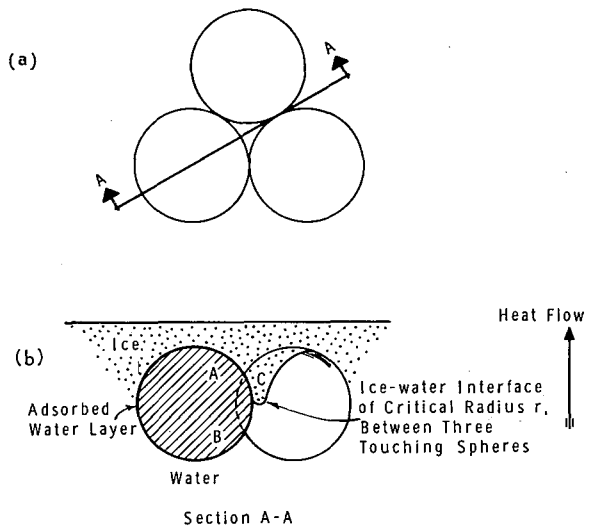

SCHEMATIC DRAWING OF ICE-WATER INTERFACE PRIOR TO PROPAGATING THROUGH PORE RESTRICTION BETWEEN THREE TOUCHING SPHERES

Fig. 1. (a) Spheres in close-pack array
(b) Schematic drawing of ice-water interface prior to propagating through pore restriction between three touching spheres

The critical radius of curvature at which a non-wetting phase displaces a completely wetting phase through the triangular shaped hole between three touching spheres has recently been investigated experimentally by Everett and Haynes (1965). It may be noted that geometrically the radius of the smallest sphere that can pass through such a hole is given by

$$\frac{r}{r_i} \simeq 6.41 . \quad (9)$$

The reason for questioning the validity of the geometry in eq. (9) is that the interface between spheres is not a surface of revolution. Everett and Haynes determined the ratio of the sphere radius to critical radius of curvature by a series of experiments involving capillary rise between close-pack cylindrical rods, maximum bubble pressure between three spheres in mutual contact, and drainage of liquid from a pyramid of

steel balls in a cubic close-pack arrangement. It was concluded from these experiments that the critical radius of curvature was approximately

$$\frac{r}{r_i} = 5.60\,, \tag{10}$$

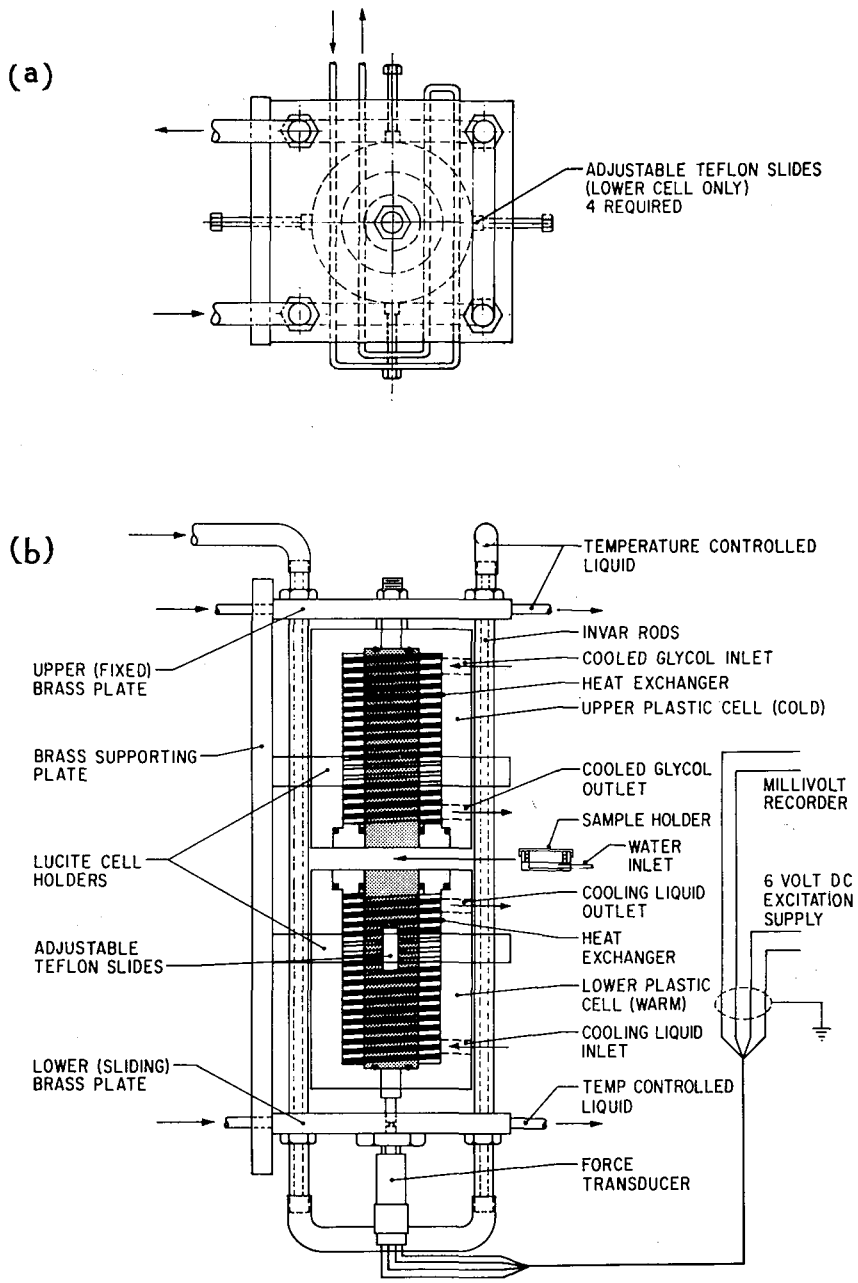

Fig. 2. (a) Heave pressure cell – top elevation
(b) Heave pressure cell – side elevation

where r is radius of spheres as before,
and r_i critical radius of curvature at the narrowest constriction of three touching spheres.

The concept of Everett and Haynes recognizes two contributions to the heaving force: one, the increase in pressure on the ice that is required for the ice to pass through a narrow constriction; the other equalling $2\pi r\sigma_{iw}$ which is taken into account in the development of eq. (8) by considering the difference in the interfacial tensions between water-solid and ice-solid.

III. Experimental Investigation

The apparatus used to measure heaving forces is shown in Figs. 2 and 3. The upper cell is the cold side and is held in a fixed position; the lower cell (warm side) rests on a sensitive force transducer, which is fixed to the lower plate. The upper and lower plates at the extremities of the cells are held together with four Invar rods 1.27 cm in diameter. Fluctuations in room temperature, which would give rise to small movements are avoided by circulating a liquid at constant temperature through the Invar rods and end plates.

The specimen is placed in a sample holder between the two cells in the centre section so that it will be in direct contact with the finned metal heat exchangers. The temperature of the glycol solution circulating round the finned heat exchangers of the two cells imposes the temperature gradient across the specimen.

The sample holder has a small porous plate at the lower end for water transmission to the specimen and the external water level keeps the specimen water-saturated during the growth of the ice lens. Temperatures, which were monitored continuously at the ends of the specimen, showed fluctuations of less than 0.01°C over periods of several days; over shorter periods the variations were considerably less. Temperature variations at the freezing front were imperceptibly small as is indicated by the constancy of heaving pressures at equilibrium.

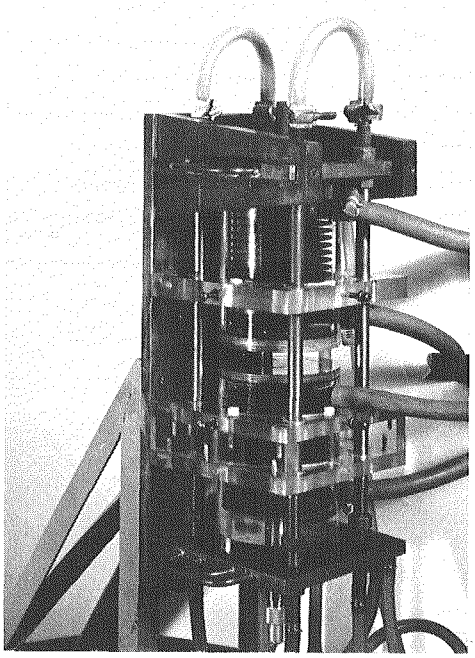

Fig. 3. *Photograph of frost heave pressure apparatus*

The experimental procedure with unconsolidated materials such as glass beads and soils was as follows. A water-saturated specimen inside a thin walled lucite sample holder was inserted between two cells and a thermal gradient established, with the upper side slightly below 0°C and the lower side slightly above the freezing temperature.

Freezing was initiated by seeding the cold side with a frosted wire. After a 24-hr period, while the pressure was increasing, the freezing plane was stationary within the sample. On stabilization the pressures were reduced to zero by adjustment of the nuts holding the upper and lower cells together. This was repeated several times until the ice lens was estimated to be about 2 mm thick. Maximum forces in the vertical direction were then allowed to develop fully and were monitored on a millivolt recorder from the output of the force transducer. The whole process was repeated, each run taking several days, depending somewhat on the kind of sample used and on the magnitude of the forces developed. As would be expected, equilibrium was approached slowly as the forces approached a maximum.

During pressure build-up the temperature at each end of the specimen was not permitted to vary, so that the forces to be measured would rise only at the ice-water interface below the ice lens and not as a result of expansion of water freezing at reduced temperatures behind the ice lens.

IV. Results

Heaving pressure measurements in pads of glass beads. Glass beads were size fractionated by sedimentation in water to obtain size uniformity. Figure 4, curve A, gives the size distribution of the original stock from which the fractionations were made. The degree of variation was established by preparing smears on glass slides and photographing them at random. Some 800 to 900 beads were measured and counted in each size range to establish this variation. The results are plotted in Fig. 4.

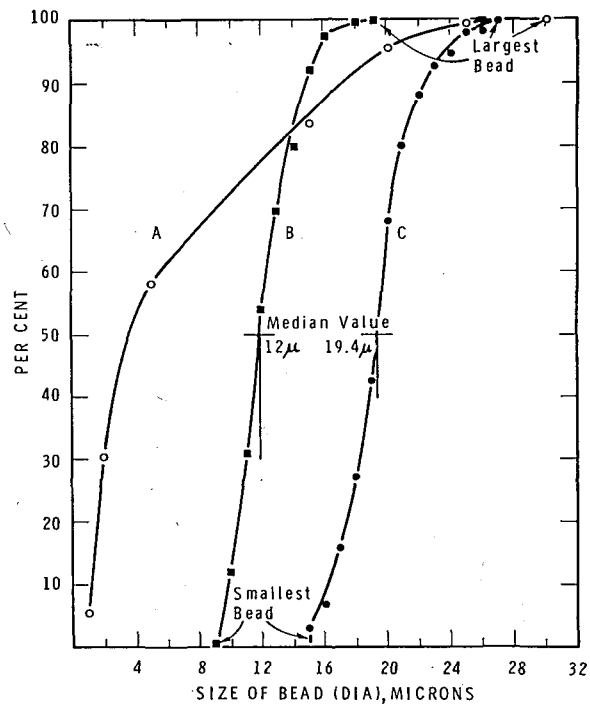

Fig. 4. Particle size distribution of unsorted and sorted glass beads

In curves B and C the median was used for calculations where the size of the particles was involved. It may be seen that the median diameter of the smaller fraction was 12.0 μ; the median diameter of the larger size fraction was 19.4 μ. The heaving force was also measured on pads of the original stock of beads.

The size varied from 9 to 19 μ (diam.) in the batch of smaller beads. From Fig. 4 it may be seen that some 10% were between 9 and 10 μ, that another 10% were from 15 to 19 μ, and that 80% were between 10 and 15 μ. The larger beads ranged in size from 15 to 27 μ, but 80% of them were between 17 and 22 μ. Five percent of the unsorted beads were smaller than 1 μ, and the largest were 30 μ.

The Everett and Haynes relation (eq. (8)) relating bead radius to heaving pressure is plotted in Fig. 5 for the two σ_{iw} values of 30 and 40. The experimental relations between bead radius and heaving pressure are indicated on the same figure. The value for the 12 μ diameter beads is an average of 10 different heaving force measurements; for the 19.4 μ size it consists of two different measurements.

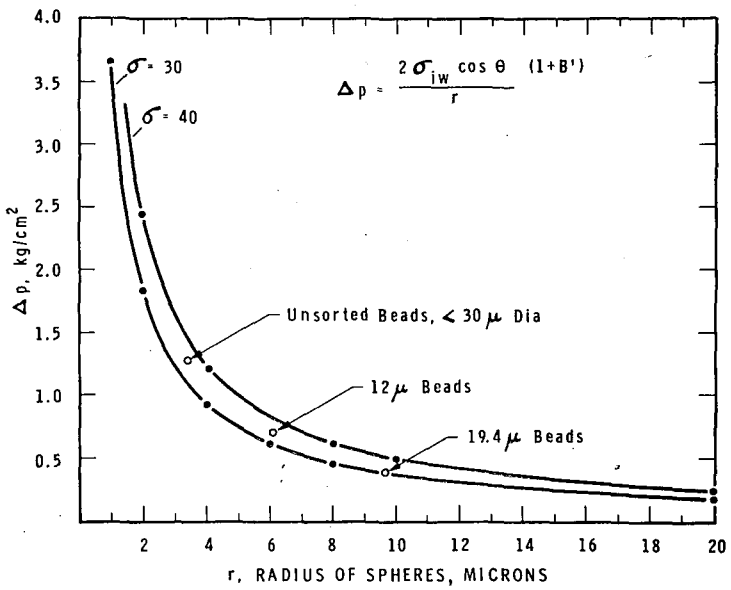

Fig. 5. Everett and Haynes equation relating heaving pressure to sphere radius

The experimental results give values for σ_{iw} of 30 and 35. At this point in the studies it was assumed that 35 is the more reliable value because the experiments were repeated a greater number of times for the 12 μ beads. Another assumption in the preparation of the bead pads was that a close-pack assemblage had been achieved, since it was for this geometry that the equation held. The pads were prepared by both jarring and tamping the sediment. Because the ice front has some capacity for rearranging the material at the freezing front, it is believed that something very close to a close-pack array was achieved at the interface between the particles and the ice lens.

The values for σ_{iw} obtained in this experiment compare favourably with the most reliable results reported in the literature from other methods of obtaining values for σ_{iw}; they give credence, therefore, to the validity of the Everett and Haynes equation.

It is believed that the experimental technique used is sufficiently refined for use in exploring ice lens pressures for materials of more complicated pore geometry. An attempt has been made to assess which pore sizes are predominant in establishing the maximum force attainable when a large pore size variation exists.

The important role of the smaller beads in the unsorted batch ranging up to 30 μ can be seen from the heaving pressures developed. The beads in Fig. 4, curve A, gave a heaving pressure of 1.28 kg/cm^2, which corresponds to bead size radius of 3.5 μ using a value of 35 for σ_{iw}.

Preliminary ice lensing pressure measurements on the surface of saturated porous solids.

Bricks. Frost action deterioration of building materials in structures has not been associated with the ice lensing mechanism until recently (Garden, 1965). It is, however, of real value to be able to understand the mechanism and so to be able to predict the possible range of stresses to which structural components can be subjected, due solely to freezing. In the context of this paper the practical significance is simply referred to, since the main objective is to relate the magnitude of the heaving stresses due to lens growth with the pore geometry.

Four bricks, as received from the manufacturer, have been studied. Two were prepared by the extrusion method, one was a "pressed" brick, and the last was a soft mud variety. Samples were cut to fit the sample holder of the heaving pressure apparatus described previously. The specimens were short cylinders 1.905 cm diameter and 0.635 cm long. The samples were taken at least 1.27 cm from any outside surface in order to avoid skin effects.

Sample preparation simply involved water saturation under vacuum. At the completion of the ice lens pressure measurements the same specimens were oven-dried and again saturated under vacuum in order to obtain total porosity. Finally, they were oven-dried and their pore size distribution determined down to 0.1 μ (diam.) with a mercury porosimeter.

The freezing technique was much the same as that described earlier, except that the ice lens was grown at the surface. The brick samples were not, in fact, frozen, but were merely in contact with a growing ice lens. Again, the crystallization of the water was induced with a frosted wire. The pressure was kept sufficiently low for a lens from 2 to 4 mm to develop rapidly, after which maximum forces were allowed to develop.

For the purpose of calculating the critical size of the pores involved a pore geometry has been assumed consisting of cylindrical capillary openings to the surface. The equation

$$p = \frac{2\sigma_{iw}}{r_i}, \tag{11}$$

is assumed to apply, where r_i is the radius of the pore constriction of the brick in direct contact with the ice lens.

Based on the area exposed to the ice and the heaving force measured experimentally, the heaving pressure calculated was 0.95 kg/cm^2 for the soft mud brick; 1.75 kg/cm^2 for the pressed brick; 2.12 kg/cm^2 for one extruded type; and 1.84 kg/cm^2 for the other.

The pore size distribution for the bricks is shown in Fig. 6; other pertinent information is given in Table 1. It may be noted that the porosimeter that was used is capable of filling pores down to 0.1 μ diameter and gives almost complete saturation for the bricks studied.

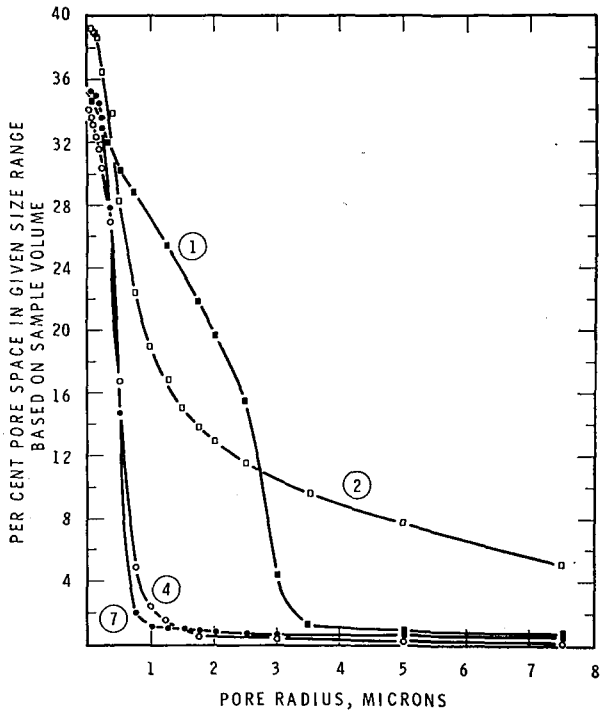

Fig. 6. Pore size distribution curves for bricks

Table 1. Percentage of pore volume and pore size properties of bricks

Brick identity	Total pore vol. of sample vol. (%)	Pore vol. greater than 0.05 size* (%)	Limiting pore size* active in lensing by eq. (11) (μ)	Pore size smaller than active in lensing (%)
1 soft mud	37.73	34.66	0.75	$\simeq$ 9
2 pressed	42.68	39.13	0.41	$\simeq$11
4 extruded	34.11	33.92	0.34	$\simeq$ 7
7 extruded	37.42	35.08	0.39	$\simeq$11

* radius of pores

The limiting radii calculated from heaving pressures did not vary greatly from brick to brick. Bricks Nos. 1 and 2, which were the soft mud and pressed varieties, had a larger percentage of pores in the large size range and these gave lower heaving pressures, particularly brick No. 1. Almost all of the pores in the two extruded bricks were smaller than 1 μ radius.

The last column in Table 1 shows the approximate percentage volume, consisting of pores smaller than the pore size calculated from the maximum heaving pressure.

This shows the importance of the smaller pores in assuming an active role in the ice lensing mechanism. The maximum pressure measured did not in any of the cases studied correspond to the smallest pores of the bricks.

Other porous materials. Ice lens heaving pressures were measured also in a sandstone and in a cement mortar. The pore size distribution down to 0.05 μ radius is given in Fig. 7. Equation (11) gave the limiting pore size radius active in heaving as 0.20 μ for the cement mortar. Comparing total pore volume with the volume of pores greater than 0.05 μ shows that half the total volume of pores in the cement mortar is less than 0.05 μ. In sandstone, limiting heaving radius 0.20, only 4% of the total pore volume was contained in pores smaller than 0.05 μ. The heaving pressures measured in the cement mortar were 3.51 kg/cm^2 and in the sandstone, 3.57 kg/cm^2.

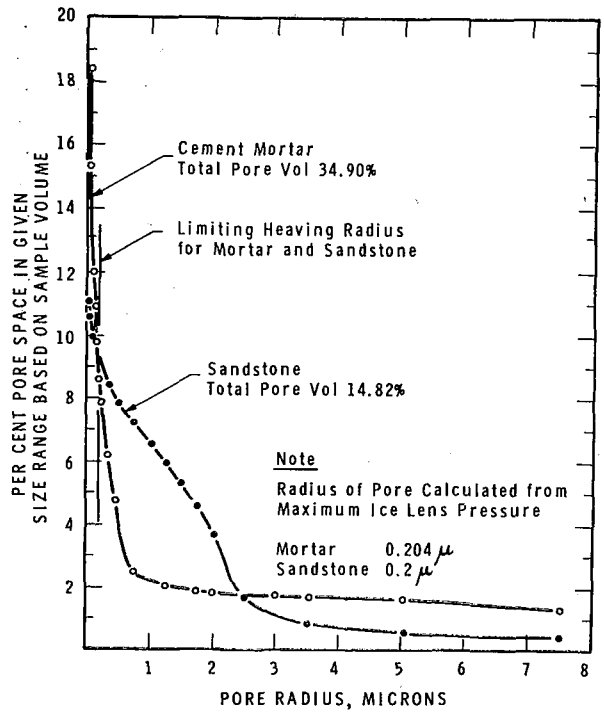

Fig. 7. Mercury porosimeter pore distribution curves for sandstone and cement mortar

Ice lensing pressures in silty soil. This particular soil, described elsewhere (Penner, 1960), has been shown to be highly frost-susceptible. It contains about 9% clay size, 43% silt, and 48% sand. Samples were prepared at two different densities to compare behaviour at radically different pore size ranges. The less dense sample (1.87 g/cm^3) was prepared by compaction in a normal compaction apparatus. The highly dense sample was compressed at 9 000 kg/cm^2 for 10 min in the air-dry state. The samples were then oven dried and trimmed to the correct size for the heaving measurements. They were allowed to saturate from one direction prior to the start of freezing.

Figure 8 shows mercury porosimeter values for both densities in the air-dry state, and shows the radically different porosities and pore size distributions for the two

es. The total pore volume determined by water saturation was 32.0% of the sample volume for the compacted sample and 15.7% for the compressed sample. eaving pressures of 1.43 kg/cm² for the high density sample and 1.23 kg/cm² for w density sample were measured, giving a critical pore size value, using eq. (11), and 0.6 μ, respectively. There is, therefore, some influence of density, as was previously (Penner, 1958), but because of the similarity in heaving pressures the effect appears to be derived from the finest particles.

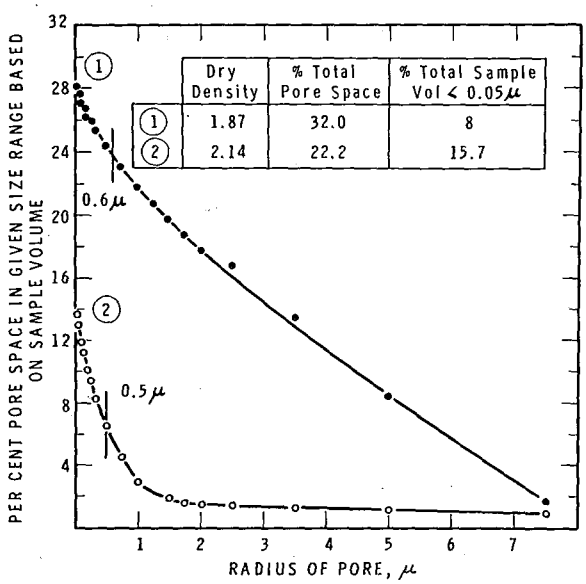

Fig. 8. Pore size distribution in silt at two densities in the oven dry state

It was obvious that on wetting the material before freezing some swelling occurred that the curves shown in Fig. 8 would not apply exactly; but in many ways this iminary method of pore size evaluation had merit. Regardless of how the sample repared, the freezing front modifies the distribution of particles to some extent, as been shown by Corte (1962), and some doubt remains as to how applicable bulk perties are to the situation at the contact between the ice lens and the particles at freezing front.

V. Summary

. Pressures resulting from ice lens growth have been measured on pads of glass ds, which are believed to be sufficiently uniform to test the equation of Everett and ynes (1965). The pressures predicted from the equation correspond to experimental ving pressures and give values for σ_{iw} between 30 and 35. The most reliable value considered to be 35.

. Heaving pressure measurements with unsorted glass beads show the significance the smaller beads in producing the ultimate ice lens pressures.

. (a) Preliminary measurement of the maximum ice lens pressures on solid porous

materials such as bricks, a cement mortar, and a sandstone show that pore size distribution is a significant factor. Brick No. 1, which had a large percentage of large pores, gave considerably lower pressures. From 7 to 11% of the pore volume, based on the total volume of the samples, had a smaller radius than that corresponding to the maximum heaving pressure, using eq. (11).

(b) Of the porous solids studied cement mortar and sandstone gave the highest pressures corresponding to critical operative radii of about 0.2 μ.

(c) Pressures in a silty soil measured at two densities indicate the influence of the finest particles in establishing heaving pressures at the ice lens front in silty soils.

Acknowledgments

The author wishes to acknowledge the assistance of his many colleagues, in particular P. J. Sereda and T. Ritchie, and also D. Eldred for his patience in assisting with the many hours of measurements involved in the various experiments. This paper is a contribution from the Division of Building Research, National Research Council, Canada, and is published with the approval of the Director of the Division.

References

1) CORTE, A. E. 1962 Vertical migration of particles in front of a moving freezing plane. *J. Geophys. Res.*, **67**, 1085–1090.

2) EVERETT, D. H. and HAYNES, J. M. 1965 Capillary properties of some model pore systems with special reference to frost damage. *RILEM Bull. New Ser.*, **27**, 31–38.

3) GARDEN, G. K. 1965 Damage to Masonry Constructions by the Ice-Lensing Mechanism. Presented at the RILEM/CIB Symposium on "Moisture Problems in Buildings," Helsinki, Finland, 8 pp.

4) PENNER, E. 1957 Soil moisture tension and ice segregation. *Highway Res. Board Bull.* **168**, 50–64.

5) PENNER, E. 1958 Pressures developed in a granular system as a result of ice-segregation. *Highway Res. Board Special Rept.*, **40**, 191–199.

6) PENNER, E. 1960 The importance of freezing rate in frost action in soils. *Proc. Amer. Soc. for Testing and Materials*, **60**, 1151–1165.

7) PENNER, E. 1965 Frost heaving in soils. Proceedings of the Permafrost, International Conference, *Nat. Acad. Sci.-Nat. Res. Council, Publ.* **1287**, 197–202.

8) SILL, R. C. and SKAPSKI, A. S. 1956 Method for the determination of the surface tension of solids, from their melting points in thin wedges. *J. Chem. Phys.*, **24**, 644–651.

AUTHOR INDEX

The boldface figures indicate the theme of the group where the author's paper belongs and the following lightface figures indicate the first page of the paper.

The correspondence between the boldface figure and the theme.

1: Physical Properties of Ice (Part 1),
2: Physical Properties of Sea Ice (Part 1),
3: Physical Properties of Deposited Snow (Part 2),
4: Mechanism of Avalanche (Part 2),
5: Physical Properties of Frost Heaving (Part 2),